Brain activity associated with emotion regulation predicts individual differences in working memory ability

Scarlett B. Horner[1], Roshni Lulla[2], Helen Wu[2], Shruti Shaktivel[2], Anthony Vaccaro[2], Ellen Herschel[2], Leonardo Christov-Moore[2], Colin McDaniel[2], Jonas Kaplan[2,*], Steven G. Greening[1,*]

[1]Department of Psychology, Brain and Cognitive Sciences, University of Manitoba, 190 Dysart Road, Winnipeg, MB R3T 2N2, Canada

[2]Department of Psychology, Brain and Cognitive Science, University of Southern California, 3620 McClintock Avenue, Los Angeles, CA 90089, United States

*Corresponding authors: Steven G. Greening, steven.greening@umanitoba.ca; Jonas Kaplan, jtkaplan@usc.edu

Citation:

Horner, S.B., Lulla, R., Wu, H. *et al.* Brain activity associated with emotion regulation predicts individual differences in working memory ability. *Cogn Affect Behav Neurosci* (2024). https://doi.org/10.3758/s13415-024-01232-6

Keywords

Emotion Regulation; Working memory; DLPFC; FMRI; Emotion

Abstract

Previous behavioral research has found that working memory is associated with emotion regulation efficacy. However, there has been mixed evidence as to whether the neural mechanisms between emotion regulation and working memory overlap. The present study tested the prediction that individual differences on the working memory subtest of the Weschler Adult Intelligence Scale (WAIS-IV) could be predicted from the pattern of brain activity produced during emotion regulation in regions typically associated with working memory such as the dlPFC. One-hundred-and-one participants completed an emotion regulation fMRI task in which they either viewed or reappraised negative images. Participants also completed working memory test outside the scanner. A whole brain covariate analysis contrasting the reappraise negative and view negative BOLD response found that activity in the right dorsal lateral prefrontal cortex (dlPFC) positively related to working memory ability. Moreover, a multivoxel pattern analysis (MVPA) approach using 10-fold cross validated support vector regression in ROIs associated with working memory, including bilateral dlPFC, demonstrated we could predict individual differences in working memory ability from the pattern of activity associated with emotion regulation. These findings support the idea that emotion regulation shares underlying cognitive processes and neural mechanisms with working memory, particularly in the dlPFC.

Introduction

The ability to change or maintain one's emotional state is critical to wellbeing (Gross, 1998). An example of this ability, referred to as emotion regulation, is reappraisal, which involves changing one's thoughts or interpretations of an emotional stimulus (Gross, 1998, 2002). The Selection, Optimization, and Compensation with Emotion Regulation (SOC-ER) model posits that certain cognitive processes are required to successfully regulate an emotional stimulus (Opitz et al., 2012; Urry & Gross, 2010), a skill also referred to as emotion regulation efficacy (Greening et al., 2014). Working memory, which involves the active maintenance, manipulation, and updating of information (Miyake et al., 2000) may be one of the key underlying cognitive process necessary for emotion regulation.

There have been several behavioral demonstrations of the association between working memory and emotion regulation, particularly for reappraisal. Research has found that executive function, and particularly working memory, is associated with behavioural emotion regulation efficacy (W. Hofmann et al., 2012; Schmeichel & Tang, 2015). In addition, people who reappraise more frequently have higher working memory capacity (Jasielska et al., 2015). Performance on working memory tasks has been shown to be positively associated with behavioural reappraisal efficacy, defined as the difference in performance between reappraisal and view trials (Hendricks & Buchanan, 2016; Opitz et al., 2014), and working memory training appears to increase emotion regulation success (Schmeichel & Tang, 2015; Schweizer et al., 2013). Such studies suggest a causal relationship between working memory and emotion regulation, with improved working memory leading to improved emotion regulation. Emotional stimuli can also disrupt performance on a task with high working memory load, while having no effect on a task with low working memory load (Tavares et al., 2016), which suggests that the same resources required for working memory are also involved in regulation of the emotional

distractor. In addition, emotion dysregulation, such as people's experiences of post-traumatic stress disorder, is also associated with worse performance on working memory tasks (Morey et al., 2009). Together, these behavioral findings suggest that emotion regulation may depend on the same cognitive processes as working memory.

Nevertheless, findings from neuroimaging studies of emotion regulation are more uncertain as to whether the brain regions associated with emotion regulation overlap with those regions associated with working memory (Denny et al., 2015; Goldin et al., 2008; Kanske et al., 2011; Lee & Xue, 2018; Morawetz et al., 2016; Ochsner et al., 2004). This research suggests one of two possibilities. One possibility is that working memory and emotion regulation are influenced by the same neural processes. Research consistently finds that reappraisal of negative images is associated with greater activity in frontal regions associated with working memory, including the dorsolateral PFC (dlPFC) and the dorsomedial PFC (dmPFC) as compared to simply viewing negative images (Buhle et al., 2014; Ochsner et al., 2012). Individual differences in behavioural emotion regulation efficacy (i.e., trial-by-trial self-reported negative affect for reappraise versus attend negative trials) is positively correlated with dlPFC activity (Greening et al., 2014), though in that study no measure of working memory was conducted. Other research finds that working memory performance along with dlPFC activity can be disrupted by emotional distractors (Dolcos & McCarthy, 2006). Research has also implicated the dorsal anterior cingulate cortex (dACC) in reappraisal (Ochsner et al., 2012). Emotional working memory training affects activity in prefrontal areas, as well as activity in the anterior cingulate cortex (ACC) during emotion regulation (Schweizer et al., 2013) implying similar neural mechanisms. In a more recent demonstration of individual differences, dlPFC activity generated by a working memory task was positively correlated with self-reported use of emotional

reappraisal (Scult et al., 2017). When reappraisal is compared directly to working memory tasks deployed during distraction-based emotion regulation, both reappraisal and working memory involve significant activation of dlPFC and dmPFC/dACC (Kanske et al., 2011; McRae et al., 2010). The dmPFC/dACC in particular seems to be involved in emotional working memory (Smith et al., 2018). However, this overlap in activation during working memory and reappraisal, and the inference of shared neural mechanisms, was derived from conjunction analyses. Unfortunately, it is possible to have overlapping brain activation from a conjunction analysis of two conditions despite distinct neural representations of the two conditions, as demonstrated using a multivoxel pattern analysis (MVPA) approach (Woo et al., 2014).

The preceding neuroimaging literature implies that one possibility is that the cognitive processes involved in working memory are likewise necessary for emotion regulation. However, a second possibility is that the overlap in brain regions engaged between working memory and emotion regulation efficacy is merely coincidental. For example, Lee and Xue (2018) argue that while there is overlap between emotion regulation and working memory in areas of the PFC, the distinct areas of the PFC associated solely with emotion regulation suggest emotion regulation and working memory do not use the same neural resources. One way to determine which of these possibilities is true is to evaluate whether MVPA of differential activity during reappraise versus look trials of an emotion regulation task (i.e., neural emotion regulation efficacy) can be used to predict individual differences in behavioural performance on a working memory task. MVPA with cross-validation offers one solution to the limitations of earlier univariate neuroimaging research (Gabrieli et al., 2015). Compared to univariate individual difference analyses, MVPA allows for greater power, meaning less participants are needed (Marek et al., 2022). It would allow for the unbiased evaluation of whether the task-relevant patterns of activation elicited

during emotion regulation are specifically predictive (Poldrack, 2008; Wager et al., 2011) of individual differences in working memory performance, rather than simply a coincidence. Were this to be the case, it would provide unbiased and direct evidence that performance during emotion regulation is underpinned by working memory.

In general, we predicted that brain activity associated with emotion regulation efficacy (i.e., the differential brain activity of reappraise negative trials versus view negative trials) in frontoparietal areas would be predictive of individual differences in working memory. To test this prediction, we first evaluated whether a behavioural measure of working memory covaries with brain activity associated with emotion regulation efficacy using a whole-brain univariate analysis. Second, we used MVPA on regions-of- interest (ROIs) commonly implicated in working memory combined with ten-fold cross-validated support vector regression analysis (Gabrieli et al., 2015). This allowed us to test the novel hypothesis that individual differences in behavioural working memory can be predicted in an unbiased manner from the pattern of brain activity produced during emotion regulation in frontoparietal regions associated with working memory such as dlPFC.

Methods

Participants

One hundred and ten participants were recruited from the general population in the Los Angeles area. Of the participants, four were removed for not completing the emotion regulation task, and five were removed for not completing the WAIS. As a result, 101 participants (62 female, 39 male) were included in the analysis. Participants were between the ages of 18 and 55 (mean age = 26.24 years, SD = 9.06). Participants were English speakers, had normal or corrected-to-normal vision, and had no history of mental illness. Participants provided written informed consent and were screened for MRI safety prior to the experiment. All study protocols

were approved in accordance with the Institutional Review Board approval guidelines provided by the University of Southern California.

Procedure

The data analyzed here are part of a larger study with independent research questions and hypotheses, which focus on the relationship between general intelligence and emotional intelligence. In the scanner, the emotion regulation task was one of four tasks relating to the four component model of emotional intelligence. However, the present work only focuses on the relationship between emotion regulation and working memory, so only those parts of the procedure will be discussed. Participants entered the MRI scanner and completed an emotion regulation task. Before the task, there was an initial fixation cross rest period of 6000 ms. In each trial, the image and an instruction below the image appeared on screen for 8000 ms. In the regulate negative condition, participants were instructed to down-regulate their emotional responses using reappraisal. In the regulate negative condition, the instruction read "Reduce," while in the view negative and view neutral conditions, the instruction read "Look." Instructions for the regulate negative condition were as followed: "When you are prompted to Reduce, you should try to change how you feel when you see each picture by searching for an alternative interpretation of what you see. For example, you might imagine ways the situation could improve for the better, or identify aspects of the situation that are not as bad as they seem, or possibly think of what you are seeing from another perspective. Please do not look away from the picture or try to distract yourself from it. We will now look at an example together and discuss how you might change your feelings about it." In the view negative condition, participants passively viewed the negative images. In the view neutral condition, participants passively viewed the neutral images. Instructions for the view conditions were as follows: "When you are prompted to Look, you should simply take in the image and try to imagine how

you would feel seeing it in real life." Afterwards, the image disappeared, and they rated how negatively the image made them feel on a sliding Likert scale of 0-5 (0 being "not strong" and 5 being "very strong"), which remained on the screen for 5000 ms, or until participants locked in their responses. Then, there was a rest jitter period of 3000-5000 ms before the next trial. The main task block consisted of 40 trials, with 15 regulate negative trials, 15 view negative trials, and 10 view neutral trials (See Figure 1). There was also a practice block of four trials, in which participants were instructed to look during the first two trials and reappraise during the last two trials. Images were sourced from the internet (such as the r/mildlydisgusting subreddit on reddit.com) and included negative images meant to induce mild, but not strong, disgust and neutral images containing scenes and objects (behavioral results from this study will confirm that subjects were able to successfully regulate their emotional responses to the stimuli). Thumbnails and ratings of the images are included in the supplemental materials. Negative images were randomly assigned to regulate negative and view negative conditions for each participant.

The experiment was completed at the MRI facility at University of Southern California using a 3T Siemens scanner with a 32-channel head coil. A T1-weighted magnetization-prepared rapid gradient-echo whole brain was used to acquire anatomical images (repetition time: 2300 ms, echo time: 2.26 ms, voxel size 1-mm isotropic voxels, flip angle 9°). Functional images were acquired in one run with a T2*-weighted gradient-echo sequence (repetition time: 2000 ms, echo time: 25 ms, 41 transverse 3-mm slices, flip angle 90°).

To measure working memory, Participants completed the WAIS-IV (Wechsler, 2008) in a second session outside the scanner. The WAIS-IV measures cognitive control and consists of four subcomponents: working memory, processing speed, verbal comprehension, and perceptual reasoning. Only the working memory component is utilized in present study. The working

memory tasks included a digit span task and an arithmetic task. In the digit span task, participants were instructed to repeat a series of digit strings either forwards or backwards (digit span sequencing was not used). In the arithmetic task, the instructor read out a word problem that the participant then was asked to solve. Working memory performance was scored using the WAIS-IV protocol (Wechsler, 2008).

Analysis

Behavioral Analyses

Behavioral analyses included a paired samples t-test, which was run to determine differences in a participants' ratings during the reappraise negative and view negative conditions. Additionally, a correlation analysis was run to show the association between the difference in ratings between reappraise negative and view negative conditions and working memory performance.

MRI Preproccesing

For each participants' emotion regulation run, fMRIPrep (version 1.1.22) was performed for preprocessing. What follows is a boilerplate from fMRIprep, distributed under the CC0 license:

First, a reference volume and its skull-stripped version were generated using a custom methodology of fMRIPrep. A B0-nonuniformity map (or fieldmap) was estimated based on a phase-difference map calculated with a dual-echo GRE (gradient-recall echo) sequence, processed with a custom workflow of SDCFlows inspired by the epidewarp.fsl script and further improvements in HCP Pipelines (Glasser et al., 2013). The fieldmap was then co-registered to the target EPI (echo-planar imaging) reference run and converted to a displacements field map (amenable to registration tools such as ANTs) with FSL's fugue and other SDCflows tools. Based on the estimated susceptibility distortion, a corrected EPI (echo-planar imaging) reference was calculated for a more accurate co-registration with the anatomical reference. The BOLD

reference was then co-registered to the T1w reference using bbregister (FreeSurfer) which implements boundary-based registration (Greve & Fischl, 2009). Co-registration was configured with six degrees of freedom. Head-motion parameters with respect to the BOLD reference (transformation matrices, and six corresponding rotation and translation parameters) are estimated before any spatiotemporal filtering using MCFLIRT (FSL 5.0.9, Jenkinson et al., 2002). BOLD runs were slice-time corrected to 0.966s (0.5 of slice acquisition range 0s-1.93s) using 3dTshift from AFNI 20160207 (Cox & Hyde, 1997, RRID:SCR_005927). The BOLD time-series (including slice-timing correction when applied) were resampled onto their original, native space by applying a single, composite transform to correct for head-motion and susceptibility distortions. These resampled BOLD time-series will be referred to as preprocessed BOLD in original space, or just preprocessed BOLD. The BOLD time-series were resampled into standard space, generating a preprocessed BOLD run in MNI152NLin2009cAsym space. First, a reference volume and its skull-stripped version were generated using a custom methodology of fMRIPrep. Automatic removal of motion artifacts using independent component analysis (ICA-AROMA) (Pruim et al., 2015) was performed on the preprocessed BOLD on MNI space time-series after removal of non-steady state volumes and spatial smoothing with an isotropic, Gaussian kernel of 6mm FWHM (full-width half-maximum). Corresponding "non-aggresively" denoised runs were produced after such smoothing. Additionally, the "aggressive" noise-regressors were collected and placed in the corresponding confounds file. Several confounding time-series were calculated based on the preprocessed BOLD: framewise displacement (FD), DVARS and three region-wise global signals. FD was computed using two formulations following Power (absolute sum of relative motions (Power et al., 2014)) and Jenkinson (relative root mean square displacement between affines (Jenkinson et al., 2002)). FD

and DVARS are calculated for each functional run, both using their implementations in Nipype (following the definitions by Power et al. 2014). The three global signals are extracted within the CSF, the WM, and the whole-brain masks. Additionally, a set of physiological regressors were extracted to allow for component-based noise correction (CompCor, Behzadi et al., 2007). Principal components are estimated after high-pass filtering the preprocessed BOLD time-series (using a discrete cosine filter with 128s cut-off) for the two CompCor variants: temporal (tCompCor) and anatomical (aCompCor). tCompCor components are then calculated from the top 2% variable voxels within the brain mask. For aCompCor, three probabilistic masks (CSF, WM and combined CSF+WM) are generated in anatomical space. The implementation differs from that of Behzadi et al. in that instead of eroding the masks by 2 pixels on BOLD space, the aCompCor masks are subtracted a mask of pixels that likely contain a volume fraction of GM. This mask is obtained by dilating a GM mask extracted from the FreeSurfer's aseg segmentation, and it ensures components are not extracted from voxels containing a minimal fraction of GM. Finally, these masks are resampled into BOLD space and binarized by thresholding at 0.99 (as in the original implementation). Components are also calculated separately within the WM and CSF masks. For each CompCor decomposition, the k components with the largest singular values are retained, such that the retained components' time series are sufficient to explain 50 percent of variance across the nuisance mask (CSF, WM, combined, or temporal). The remaining components are dropped from consideration. The head-motion estimates calculated in the correction step were also placed within the corresponding confounds file. The confound time series derived from head motion estimates and global signals were expanded with the inclusion of temporal derivatives and quadratic terms for each (Satterthwaite et al., 2013). Frames that exceeded a threshold of 0.5 mm FD or 1.5 standardised DVARS were annotated as motion

outliers. All resamplings can be performed with a single interpolation step by composing all the pertinent transformations (i.e. head-motion transform matrices, susceptibility distortion correction when available, and co-registrations to anatomical and output spaces). Gridded (volumetric) resamplings were performed using antsApplyTransforms (ANTs), configured with Lanczos interpolation to minimize the smoothing effects of other kernels (Lanczos, 1964). Non-gridded (surface) resamplings were performed using mri_vol2surf (FreeSurfer).

The above boilerplate text was automatically generated by fMRIPrep with the express intention that users should copy and paste this text into their manuscripts *unchanged*. It is released under the CC0 license.

Afterwards, spatial smoothing using a Gaussian kernel of FWHM 5.0mm was applied, as smoothing does not negatively affect MVPA results (Op de Beeck, 2010) and may actually improve the sensitivity of multivariate analyses (Hendriks et al., 2017). Noise regressors were removed all at once using a level 1 general linear model on each participant in FSL (Woolrich et al., 2001). Specifically, this initial level 1 analysis regressed out noise by including the following nuisance regressors from the fMRIprep preprocessing: six rigid-body motion regressors, every component identified as noise by ICA-AROMA, and the first principle component from the restricted white matter + gray matter mask created by compCor. The resulting cleaned residual file was used for the primary analysis described below.

Whole Brain Analysis

The cleaned residual data underwent time-series statistical analyses as carried out using FILM with local autocorrelation correction (Woolrich et al., 2001). We ran a second level 1 analysis on the cleaned residual data that included three regressors of interest and three regressors of no interest. The regulate negative, view negative, and view neutral regressors were included as regressors of interest, which were event-related and lasted for the eight seconds (i.e.,

the duration of the image presentation and the period during which participants carried out the instructed task condition). The regulate negative ratings, view negative ratings, and view neutral ratings regressors were included as regressors of no interest, which were event related and lasted up to five seconds, contingent on reaction time during the Likert epoch. The double gamma hemodynamic response function (HRF) was used to convolve the basic waveform for all regressors. Temporal derivatives of all task-related regressors were included. Contrasts measured were the regulate negative condition, the view negative condition, the view neutral condition, and a contrast of regulation efficacy, regulate negative – view negative difference.

The second-level analysis, which included one run for each subject, were carried out using a fixed effects model, by forcing the random effects variance to zero in FLAME (FMRIB's Local Analysis of Mixed Effects, Beckmann et al., 2003; Woolrich, 2008; Woolrich et al., 2004).

We then performed standard univariate and covariate group analyses using FLAME stage 1 (Beckmann et al., 2003; Woolrich, 2008; Woolrich et al., 2004). Z (Gaussianised T/F) statistic images were thresholded using clusters determined by $Z>3.1$ and a (corrected) cluster significance threshold of $p = 0.05$ (Worsley, 2001). In the whole-brain covariate analysis, WAIS-IV working memory scores were used as an additional predictor. The covariate analysis used WAIS-IV working memory scores to predict differences in BOLD activity between regulate negative and view negative conditions. In other words, the covariate analysis identified brain areas that responded during reappraising that are predictive of working memory performance. Further details of the univariate analyses can be found at https://neurovault.org/collections/IHXZNJXZ.

Multivariate Analysis

Next, we used multi-voxel pattern analysis (MVPA) with a continuous support vector regression (SVR) analysis using a linear kernel to determine if we could predict working

memory performance on the WAIS-IV with the regulate negative – view negative BOLD contrast. SVR is a linear regression based on support vector machines, which performs well particularly with high dimensional data, such as datasets with a high voxel counts as features (Misaki et al., 2010), or data used to determine individual differences (Zhou et al., 2021). The SVR was implemented using a stratified 10-fold cross-validation scheme (Greening & Mitchell, 2015), where the test set included 10 participants (with the exception of one set which included 11) and no participant was removed more than once. The voxels for inclusion as features were from brain areas that were selected using an ROI approach based on independent components analysis (ICA). The use of ICA was a feature reduction step, as fMRI data is notoriously overdetermined in that the number features (i.e., voxels) greatly exceeds the number of examples (i.e., participants). In particular, we were interested in areas implicated in working memory, we used feature reduction to focus on those areas typically associated with working memory. Feature reduction is a common strategy for reducing problems commonly associated with highly overdetermined datasets such as overfitting (Hughes, 1968). The ICA was conducted at the group level with Regulate Negative – View Negative contrasts using MELODIC. Following this group ICA, we selected the Independent Components (ICs) that included brain regions commonly associated with working memory. We did this by using fslcc to evaluate the interclass correlation between each IC produced and a brain map associated with working memory based on the meta-analysis results found on Neurosynth.org (Yarkoni et al., 2011). It is worth noting that while we looked for ICs that correlated with meta-analytical working memory activity from Neurosynth, our functional data was emotion regulation data and no working memory tasks were completed in the scanner. In other words, our feature reduction was blind to our primary outcome measure of the multivariate analysis, which was the WAIS working memory measure conducted outside

the scanner. Using this approach, we identified two ICs correlated with working memory. These two ICs were then turned into binary masks by thresholding the maps at a voxel-level with a z-value of 3.1, and transformed into more discreet clusters using erosion and dilation. See the results section for details on the regions identified.

For each participant and each MVPA analysis (i.e., for each of the two ROI maps and for the whole-brain analysis below), a matrix of voxels containing the emotion regulation efficacy contrast parameter estimates was made. In each fold, the training data was used to train an SVR model on the emotion regulation efficacy voxel activity to predict the working memory WAIS-IV scores of the training data; after training, the trained model was tested on the held out set of test participant data to predict the working memory WAIS-IV score of each participant in the test set. After the ten-fold cross validation, we were left with one predicted working memory WAIS-IV score per participant, which we then compared to the known working memory WAIS-IV score using root mean square error (RMSE), or the empirical RMSE. To evaluate whether the empirical RMSE was significantly lower than chance, it was compared to permutation estimated RMSEs from 1000 permutation simulations in which the working memory scores randomly shuffled amongst the participants. Further details of the multivariate analysis can be found at https://neurovault.org/collections/IHXZNJXZ.

Results

Behavioral Results

Working memory scores as measured by the WAIS-IV ranged from 83 to 145 (M= 110.8, SD = 12.27) and were distributed normally. A paired samples t-test determined that there was a significant difference in ratings of negativity between the reappraise negative condition (M = 2.553, SD = 0.531) and the view negative condition (M = 3.237, SD = 0.567), t(100) = -11.287, *p*

< .001, Cohen's d' = -1.245 (see Figure 2a). In addition, a Pearson's correlation analysis showed a negative correlation between reappraisal efficacy (defined as Reappraise Negative - View Negative) and working memory score, suggesting that a more negative difference between Reappraise Negative and View Negative is associated with greater working memory performance r(99) = -0.306, *p* = .0018 (see Figure 2b).

Univariate Analysis

We found significantly greater activity to Regulate Negative compared to View Negative in bilateral aspects of the orbital frontal cortex, bilateral aspects of the ventrolateral prefrontal cortex, bilateral aspects of the frontal poles, the left superior frontal gyrus, the left middle frontal gyrus, the left inferior frontal gyrus, the left dorsal lateral prefrontal cortex, and aspects of the right middle temporal gyrus. We observed significantly greater activity to View Negative compared to Regulate Negative trials in aspects of the right premotor cortex, the right middle/inferior temporal gyrus, the right temporal lobe, and the left somatosensory cortex (Table 1).

Covariate Analysis

The results of the contrasts between Regulate Negative and View Negative with working memory WAIS score as a predictor above a threshold of 3.1 can be seen in Figure 3. Individual differences in working memory were positively associated with greater differential activity in the right dlPFC/right middle frontal gyrus during the Regulate versus View Negative condition (Table 2). A similar result was found when controlling for age and gender variables. Despite the circularity and non-independence of performing analysis on voxels already selected to show a correlation (Kriegeskorte et al., 2009), to understand whether the effect was being driven by the Reappraise Negative trials, the View Negative trials, or both we created scatterplots and

performed follow-up correlational analysis on the dlPFC cluster to visualize the effect (Middle of Figure 3). This visualization suggested that whereas greater activity during the regulate negative condition was associated with greater working memory scores ($p = .007$), greater activity in the view negative condition was not associated with working memory scores ($p = .945$).

As an exploratory analysis, we also re-ran the covariate analysis with the initial cluster threshold reduced to 2.3. As the primary covariate analysis revealed, working memory was associated again with greater differential the activity in the right dlPFC. However, we also observed that the left angular gyrus, the bilateral dorsomedial prefrontal cortex (Paracingulate Gyrus), and the left middle temporal gyrus (see Figure 3) were all positively associated with working memory WAIS-IV scores.

Lastly, we also conducted exploratory covariate analyses on each condition independently to follow up on the above with a cluster threshold of 3.1. This revealed a significant positive association between working memory and the regulate negative condition, such that greater working memory predicited greater activity in the right dlPFC and bilateral occipital cortex (Table 2). There was no negative association between working memory and activity during regulate negative. There were also no significant clusters for either positive or negative associations between working memory and activity in the view negative condition.

Multivariate Analysis

The group ICA analysis produced two ICs that were most implicated in working memory. The first IC (ROI 1, Pearson's $r = .28$) included bilateral frontoparietal regions associated with working memory, including bilateral dlPFC, dmPFC, and dACC, and areas of the superior and inferior parietal cortex. The second IC (ROI 2, Pearson's $r = .30$) also included aspects of the

bilateral dlPFC as well as parts of the lateral occipital cortex. See Figure 4 for detailed ROI maps.

For the MVPA, we completed no feature selection other than using the masks containing the ROIs (See Figure 4 for anatomical extent of the mask and the resulting weights from the analysis; further details regarding linear weights can be found at https://neurovault.org/collections/IHXZNJXZ). Using ROI 1, we found that differential brain activity associated with emotion regulation efficacy was able to predict individual working memory scores significantly better than chance (RMSE = 11.893, p = .014). In addition, we found that differential brain activity associated with emotion regulation efficacy was able to predict individual working memory scores significantly better than chance using ROI 2 (RMSE = 12.098, p = .042). We found a similar pattern of results after combining both ROIs into a single mask (RMSE = 11.954, p = .034) (See Figure 5). However, when performing a whole brain analysis with 10% feature selection, our results were only marginally significant (RMSE = 12.079, p = .079).

Discussion

The purpose of this study was to determine if working memory and emotion regulation share similar underlying neurocognitive processes. To test this possibility, differential brain activity during reappraisal versus viewing of negative images was used to predict individual differences in working memory ability. First, we conducted an analysis which revealed that working memory significantly covaried with brain activity resulting from the contrast between reappraising images and viewing negative images in the right dorsolateral prefrontal cortex. We also completed an ROI-based MVPA analysis to determine whether activity during emotion regulation predicted working memory ability using stratified 10-fold cross validation. This

analysis demonstrated that ROI 1, which included bilateral dlFPC, dmPFC/dACC, and parietal regions, and ROI 2, which included bilateral dlPFC and occipital regions, both predicted working memory ability above chance.

The behavioral results of the presented study demonstrated that working memory performance, as measured using the WAIS-IV score, is positively correlated with emotion regulation efficacy as measured with average self-reported reappraise negative ratings minus average view negative ratings. Specifically, emotion regulation efficacy was positively correlated with working memory performance. The behavioral findings replicate previous research showing that working memory predicts reappraisal performance when measured by a keep track task (Hendricks & Buchanan, 2016) as well as the digit span portion of the WAIS-IV (Opitz et al., 2014). By having participants complete all working memory components of the WAIS-IV (i.e. digit span and arithmetic task), we replicate and further generalize of the association between reappraisal efficacy and working memory.

The first important finding of the present study is the covariate analysis demonstrating that the differential activity between reappraising and viewing negative images in the right dlPFC positively covaried with individual working memory scores. Although to our knowledge this is a novel finding not previously reported in the literature, it corroborates previous research that the dlPFC is an area of interest in both reappraisal and working memory tasks (Kanske et al., 2011; McRae et al., 2010; Ochsner et al., 2012). Previous research has also shown that dlPFC activity produced using a working memory task predicts self-reported reappraisal frequency (Scult et al., 2017). Moreover, other research has observed that differential dlPFC activity associated with reappraising negative versus looking at negative stimuli is positively correlated with emotion regulation success (Kanske et al., 2011; McRae et al., 2010). Together with the previous

literature, the present results support the idea of the right dlPFC being implicated in both emotional reappraisal and working memory, but also further suggests that the neural mechanisms associated with successful emotion regulation are at least correlated with working memory.

We also observed that activity in additional fronto-parietal regions (bilateral dmPFC and angular gyrus) positively covaried with working memory. Although these findings were the result of the more liberal exploratory analysis using a cluster forming threshold of Z=2.3, they are consistent with the inference that brain regions commonly associated with working memory ability (Curtis & D'Esposito, 2003; Dolcos et al., 2013) are contributing to the process of emotion regulation. Likewise, previous research comparing brain activity elicited during reappraisal versus working memory-based distraction of emotional pictures found similar activity in the dmPFC and lateral parietal regions (Kanske et al., 2011; McRae et al., 2010).

Extending beyond the covariate analysis, most important and notably, we also observed that MVPA with stratified 10-fold cross validation using the pattern of brain activity in our two ROIs on the differences between reappraising and viewing negative images could be used to predict working memory performance on the WAIS-IV significantly above chance. Differential brain activity while reappraising and viewing negative images predicted working memory when using ROI 1, ROI 2, and a combined mask of ROIs 1 and 2. Both ROI 1 and 2 included bilateral aspect of dlPFC and aspects of dmPFC/dACC. This pattern is in line with previous research showing that brain activity during a working memory task is correlated with how often one used reappraisal (Scult et al., 2017). Rather than simply demonstrating the reverse of Scult et al. (2017), our finding further contributes to the research by including a biological measure of reappraisal efficacy (i.e., fMRI activity) rather than self-reported questionnaire data. More broadly, our novel findings extend beyond the previous correlational research by demonstrating

that individual differences in working memory can be predicted in an unbiased manner from the neural representation pattern elicited by emotion regulation.

In terms of the brain regions associated with emotion regulation and working memory, the involvement of the dlPFC was observed in both the covariate and MVPA analyses, which is consistent with previous literature (Kanske et al., 2011; McRae et al., 2010). Activity in the dlPFC is also associated with top-down processing (Blair & Mitchell, 2009), which may explain its role in the cognition-driven reappraisal. The present results implicating the dmPFC/dACC in addition to the dlPFC also coincides with previous research. For example, Schweizer et al. (2013) found that working memory training was able to improve emotion regulation as well as increase recruitment of both medial (i.e., dmPFC/dACC) and lateral areas of the prefrontal cortex during activation emotion regulation (Schweizer et al., 2013). While there is no consensus on whether the dlPFC versus the dmPFC/dACC make unique contributions to working memory and emotion regulation, there are several theories about their roles. One theory is that the dmPFC/dACC is associated with emotional appraisals (Maier et al., 2012) and emotion regulation (Greening et al., 2013; Silvers et al., 2015) alongside working memory. Alternatively, the medial prefrontal areas are associated with emotional attention and pulling resources from prefrontal areas (Pessoa, 2009). Therefore, emotional stimuli pull resources from the dlPFC typically associated with working memory, thus impairing working memory performance. Alternatively, the dmPFC/dACC may signal to the dlPFC when cognitive control or emotion regulation is necessary (Mitchell, 2011). Therefore, it is possible that emotion regulation and working memory compete for the same resources, likely those within the central executive. The central executive system plays a role in attention and performance involved in working memory (Baddeley, 2003). However, in the presence of an emotional stimulus, attention and working

memory are required in order to regulate that stimulus (Pessoa, 2009), taking from those resources. The MVPA analysis also found evidence of bilateral inferior parietal lobe being involved in working memory and emotion regulation. Prior research has found the inferior parietal lobe to be implicated in networks associated with neural emotion regulation efficacy (Morawetz et al., 2016) and but also necessary for working memory performance (Alain et al., 2008; Olson & Berryhill, 2009).

The present study is the first of our knowledge to use MVPA on emotion regulation data to predict individual differences in working memory. MVPA with cross-validation advances our knowledge of emotion regulation and working memory as it serves as a robust unbiased approach for measuring the predictive effect size of brain activity on behaviour, and therefore the generalizability of the prediction model to individual differences (Gabrieli et al., 2015; Zhou et al., 2021). It has also proved to be useful for uncovering the neurocognitive mechanisms of emotion regulation in other contexts. For example, MVPA has been used to differentiate brain activity during reappraisal from brain activity during distraction (Martins et al., 2014). MVPA has also been used to determine whether emotions were being up-regulated or down-regulated (Morawetz et al., 2016). While Martins et al. (2014) and Morawetz et al. (2016) used support vector classficiation, which is appropriate for categorical data, SVR is a useful tool for predicting continuous data such as individual differences. For example, SVR has been used previously to predict individual differences in working memory capacity (Ullman et al., 2014). By moving beyond a simple correlational or covariate analysis, and using the more robust method of MVPA with cross-validation, this study further supports the role of prefrontal areas in emotion regulation being predictive of working memory ability. In addition, our findings support the idea

that the neural mechanisms involved in working memory are quantitatively similar to those mechanisms associated with emotion regulation.

According to the modal model of emotion regulation, emotion regulation consists of situation focused, attention focused, cognition focused, and response focused stages (Gross, 2002, 2014). The cognition stage of emotion regulation is particularly important as it is the phase during which reappraisal takes place (Gross, 2002). The SOC-ER model posits that to successfully regulate emotions, cognitive processes are required to select an emotion regulation method, optimize it, and compensate for any emotion regulation failures (Opitz et al., 2012; Urry & Gross, 2010). As our findings support the notion that emotion regulation, particularly reappraisal, is underpinned by a cognitive process shared with working memory, it implies that if a person does not have the proper working memory resources, their reappraisal of the stimulus is less likely to be successful. This is of interest as cognition-based methods of emotion regulation, such as reappraisal, are considered very effective forms of emotion regulation (Gross & John, 2003). If someone is unable to properly reappraise, they may have a difficult time decreasing negative emotion and struggle with coping strategies. This emotion regulation failure, or emotion dysregulation, can occur when cognitive processes, such as working memory, are impaired. Emotion dysregulation is a cornerstone of several mental illnesses, particularly anxiety and mood disorders (S. G. Hofmann et al., 2012). In a similar vein, impaired executive function, including working memory, is associated with similar mental illnesses (Snyder et al., 2015). According to the SOC-ER model, these issues with executive dysfunction would mean a person lacks the necessary cognitive resources to regulate their emotions properly (Opitz et al., 2012), which in turn causes anxiety and mood disorders to form (S. G. Hofmann et al., 2012).

As the the present study was not preregisted, a preregistered replication is needed to determine if this finding can be found in confirmatory contexts. Different settings and participant populations will also help identify if the findings generalize. Another limitation to the study is that it is possible participants were regulating the image in the view condition, as they were instructed to respond naturally to the image, which may imply regulation, though the self-reported rating suggest otherwise. Future research could focus on whether brain activity during reappraisal affects other aspects of executive function. Aside from working memory, executive function also consists of inhibition and shifting attention, and these three aspects of executive function share some overlap (Friedman & Miyake, 2017; Miyake et al., 2000). Executive function is driven by activity in the prefrontal cortex (Friedman & Miyake, 2017), and activation in the dmPFC/dACC from emotional attention pulls prefrontal resources associated with executive function (Pessoa, 2009). This suggests that other forms of executive function (i.e. inhibition and shifting) may impact emotion regulation as well. Executive function is necessary to maintain, monitor, switch, and stop emotion regulation methods (Pruessner et al., 2020). In addition, there is evidence that other forms of executive function, inhibition and shifting, have behavioral associations with working memory (Schmeichel & Tang, 2015). Therefore, it is possible that differential emotion regulation activity may predict inhibition and switching performance. Future research could also look at the role the dlPFC plays in emotion regulation during high intensity or stressful situations, or how the dlPFC mediates the role adversity plays in emotion regulation efficacy. Previous research has found the left dlPFC is implicated in resilience in the face of adversity (Brosch et al., 2022; Cisler et al., 2013). Considering the role of the dlPFC during both reappraisal and working memory, as well as the lack of activity in the

dlPFC when looking at an emotional image it may be possible that intense negative emotions may inhibit the dlPFC, leading to poorer emotion regulation efficacy and worse resilience.

In summary, our study supports the notion that emotion regulation and working memory performance are supported by at least partially shared neurocognitive processes. This study not only further solidifies existing work by showing that working memory ability is a cognitive resource which drives instructed emotion regulation efficacy correlationally, but it also demonstrated that individual differences in working memory performance can be predicted from neural activity during emotion regulation using MVPA and cross-validation. Therefore, working memory capacity may serve as a cognitive resource necessary for emotion regulation success. This is of importance because successful emotion regulation is necessary for wellbeing.

Declarations

Funding

This work was funded by the Templeton World Charity Foundation, grant #TWCF0334, to J.K.; and supported by funding from an NSERC Discovery Grant to S.G.G.

Conflict of Interest

None of the authors have any conflicts of interest to declare.

Ethics Approval

This work was approved by the University of Southernn California IRB and University of Manitoba REB.

Consent to participate and Consent ot publication

Informed consent was received for all participants in this study.

Availability of data and materials

N/A

Code availability

N/A

References

Alain, C., He, Y., & Grady, C. (2008). The Contribution of the Inferior Parietal Lobe to Auditory Spatial Working Memory. *Journal of Cognitive Neuroscience*, *20*(2), 285–295. https://doi.org/10.1162/jocn.2008.20014

Baddeley, A. (2003). Working memory and language: An overview. *Journal of Communication Disorders*, *36*(3), 189–208. https://doi.org/10.1016/S0021-9924(03)00019-4

Beckmann, C. F., Jenkinson, M., & Smith, S. M. (2003). General multilevel linear modeling for group analysis in FMRI. *NeuroImage*, *20*(2), 1052–1063. https://doi.org/10.1016/S1053-8119(03)00435-X

Behzadi, Y., Restom, K., Liau, J., & Liu, T. T. (2007). A component based noise correction method (CompCor) for BOLD and perfusion based fMRI. *NeuroImage*, *37*(1), 90–101. https://doi.org/10.1016/j.neuroimage.2007.04.042

Blair, R. J. R., & Mitchell, D. G. V. (2009). Psychopathy, attention and emotion. *Psychological Medicine*, *39*(4), 543–555. https://doi.org/10.1017/S0033291708003991

Brosch, K., Stein, F., Meller, T., Schmitt, S., Yuksel, D., Ringwald, K. G., Pfarr, J. K., Waltemate, L., Lemke, H., Opel, N., Meinert, S., Dohm, K., Grotegerd, D., Goltermann, J., Repple, J., Winter, A., Jansen, A., Dannlowski, U., Nenadić, I., … Krug, A. (2022). DLPFC volume is a neural correlate of resilience in healthy high-risk individuals with both childhood maltreatment and familial risk for depression. *Psychological Medicine*, *52*(16), 4139–4145. https://doi.org/10.1017/S0033291721001094

Buhle, J. T., Silvers, J. A., Wager, T. D., Lopez, R., Onyemekwu, C., Kober, H., Weber, J., & Ochsner, K. N. (2014). Cognitive Reappraisal of Emotion: A Meta-Analysis of Human Neuroimaging Studies. *Cerebral Cortex*, *24*(11), 2981–2990. https://doi.org/10.1093/cercor/bht154

Cisler, J. M., James, G. A., Tripathi, S., Mletzko, T., Heim, C., Hu, X. P., Mayberg, H. S., Nemeroff, C. B., & Kilts, C. D. (2013). Differential functional connectivity within an emotion regulation neural network among individuals resilient and susceptible to the depressogenic effects of early life stress. *Psychological Medicine*, *43*(3), 507–518. https://doi.org/10.1017/S0033291712001390

Cox, R. W., & Hyde, J. S. (1997). Software tools for analysis and visualization of fMRI data. *NMR in Biomedicine*, *10*(4–5), 171–178. https://doi.org/10.1002/(SICI)1099-1492(199706/08)10:4/5<171::AID-NBM453>3.0.CO;2-L

Curtis, C. E., & D'Esposito, M. (2003). Persistent activity in the prefrontal cortex during working memory. In *Trends in Cognitive Sciences* (Vol. 7, Issue 9, pp. 415–423). Elsevier Ltd. https://doi.org/10.1016/S1364-6613(03)00197-9

Denny, B. T., Inhoff, M. C., Zerubavel, N., Davachi, L., & Ochsner, K. N. (2015). Getting over it: Long-lasting effects of emotion regulation on amygdala response. *Psychological Science*, *26*(9), 1377–1388. https://doi.org/10.1177/0956797615578863

Dolcos, F., Iordan, A. D., Kragel, J., Stokes, J., Campbell, R., McCarthy, G., & Cabeza, R. (2013). Neural correlates of opposing effects of emotional distraction on working memory and episodic memory: An event-related fMRI investigation. *Frontiers in Psychology*, *4*(JUN), 1–16. https://doi.org/10.3389/fpsyg.2013.00293

Dolcos, F., & McCarthy, G. (2006). Brain systems mediating cognitive interference by emotional distraction. *Journal of Neuroscience*, *26*(7), 2072–2079. https://doi.org/10.1523/JNEUROSCI.5042-05.2006

Friedman, N. P., & Miyake, A. (2017). Unity and diversity of executive functions: Individual differences as a window on cognitive structure. *Cortex*, *86*, 186–204. https://doi.org/10.1016/j.cortex.2016.04.023

Gabrieli, J. D. E., Ghosh, S. S., & Whitfield-Gabrieli, S. (2015). Prediction as a humanitarian and pragmatic contribution from human cognitive neuroscience. *Neuron*, *85*(1), 11–26. https://doi.org/10.1016/j.neuron.2014.10.047

Glasser, M. F., Sotiropoulos, S. N., Wilson, J. A., Coalson, T. S., Fischl, B., Andersson, J. L., Xu, J., Jbabdi, S., Webster, M., Polimeni, J. R., Van Essen, D. C., & Jenkinson, M. (2013). The minimal preprocessing pipelines for the Human Connectome Project. *NeuroImage*, *80*, 105–124. https://doi.org/10.1016/j.neuroimage.2013.04.127

Goldin, P. R., McRae, K., Ramel, W., & Gross, J. J. (2008). The neural bases of emotion regulation: Reappraisal and suppression of negative emotion. *Biological Psychiatry*, *63*(6), 577–586. https://doi.org/10.1016/j.biopsych.2007.05.031

Greening, S. G., & Mitchell, D. G. V. (2015). A network of amygdala connections predict individual differences in trait anxiety. *Human Brain Mapping*, *36*(12), 4819–4830. https://doi.org/10.1002/hbm.22952

Greening, S. G., Osuch, E. A., Williamson, P. C., & Mitchell, D. G. V. (2013). Emotion-related brain activity to conflicting socio-emotional cues in unmedicated depression. *Journal of Affective Disorders*, *150*(3), 1136–1141. https://doi.org/10.1016/j.jad.2013.05.053

Greening, S. G., Osuch, E. A., Williamson, P. C., & Mitchell, D. G. V. (2014). The neural correlates of regulating positive and negative emotions in medication-free major depression. *Social Cognitive and Affective Neuroscience*, *9*(5), 628–637. https://doi.org/10.1093/scan/nst027

Greve, D. N., & Fischl, B. (2009). Accurate and robust brain image alignment using boundary-based registration. *NeuroImage*, *48*(1), 63–72. https://doi.org/10.1016/j.neuroimage.2009.06.060

Gross, J. J. (1998). The emerging field of emotion regulation: An integrative review. *Review of General Psychology*, *2*(3), 271–299. https://doi.org/https://doi.org/10.1037/1089-2680.2.3.271

Gross, J. J. (2002). Emotion regulation: Affective, cognitive, and social consequences. *Psychophysiology*, *39*, 281–291. https://doi.org/10.1002/9780470177334.ch3

Gross, J. J. (2014). *Emotion regulation: Conceptual and empirical foundations*.

Gross, J. J., & John, O. P. (2003). Individual Differences in Two Emotion Regulation Processes: Implications for Affect, Relationships, and Well-Being. *Journal of Personality and Social Psychology*, *85*(2), 348–362. https://doi.org/10.1037/0022-3514.85.2.348

Hendricks, M. A., & Buchanan, T. W. (2016). Individual differences in cognitive control processes and their relationship to emotion regulation. *Cognition and Emotion*, *30*(5), 912–924. https://doi.org/10.1080/02699931.2015.1032893

Hendriks, M. H. A., Daniels, N., Pegado, F., & Op de Beeck, H. P. (2017). The Effect of Spatial Smoothing on Representational Similarity in a Simple Motor Paradigm. *Frontiers in Neurology*, *8*. https://doi.org/10.3389/fneur.2017.00222

Hofmann, S. G., Sawyer, A. T., Fang, A., & Asnaani, A. (2012). Emotion dysregulation model of mood and anxiety disorders. *Depression and Anxiety*, *29*(5), 409–416. https://doi.org/10.1002/da.21888

Hofmann, W., Schmeichel, B. J., & Baddeley, A. D. (2012). Executive functions and self-regulation. *Trends in Cognitive Sciences*, *16*(3), 174–180. https://doi.org/10.1016/j.tics.2012.01.006

Hughes, G. (1968). On the mean accuracy of statistical pattern recognizers. *IEEE Transactions on Information Theory*, *14*(1), 55–63. https://doi.org/10.1109/TIT.1968.1054102

Jasielska, A., Kaczmarek, L., Brońska, A., Dominiak, M., Niemier, K., Patalas, D., Sokołowski, A., & Tomczak, M. (2015). The relationship between working memory and emotion regulation strategies. *Annals of Psychology*, *18*(4), 567–578.

Jenkinson, M., Bannister, P., Brady, M., & Smith, S. (2002). Improved optimization for the robust and accurate linear registration and motion correction of brain images. *NeuroImage*, *17*(2), 825–841. https://doi.org/10.1006/nimg.2002.1132

Kanske, P., Heissler, J., Schönfelder, S., Bongers, A., & Wessa, M. (2011). How to regulate emotion? Neural networks for reappraisal and distraction. *Cerebral Cortex*, *21*(6), 1379–1388. https://doi.org/10.1093/cercor/bhq216

Kriegeskorte, N., Simmons, W. K., Bellgowan, P. S., & Baker, C. I. (2009). Circular analysis in systems neuroscience: The dangers of double dipping. *Nature Neuroscience*, *12*(5), 535–540. https://doi.org/10.1038/nn.2303

Lanczos, C. (1964). Evaluation of Noisy Data. *Journal of the Society for Industrial and Applied Mathematics Series B Numerical Analysis*, *1*(1), 76–85. https://doi.org/10.1137/0701007

Lee, T. W., & Xue, S. W. (2018). Does emotion regulation engage the same neural circuit as working memory? A meta-analytical comparison between cognitive reappraisal of negative emotion and 2-back working memory task. *PLoS ONE*, *13*(9). https://doi.org/10.1371/journal.pone.0203753

Maier, S., Szalkowski, A., Kamphausen, S., Perlov, E., Feige, B., Blechert, J., Philipsen, A., van Elst, L. T., Kalisch, R., & Tüscher, O. (2012). Clarifying the Role of the Rostral dmPFC/dACC in Fear/Anxiety: Learning, Appraisal or Expression? *PLoS ONE*, *7*(11). https://doi.org/10.1371/journal.pone.0050120

Marek, S., Tervo-Clemmens, B., Calabro, F. J., Montez, D. F., Kay, B. P., Hatoum, A. S., Donohue, M. R., Foran, W., Miller, R. L., Hendrickson, T. J., Malone, S. M., Kandala, S., Feczko, E., Miranda-Dominguez, O., Graham, A. M., Earl, E. A., Perrone, A. J., Cordova, M., Doyle, O., … Dosenbach, N. U. F. (2022). Reproducible brain-wide association studies require thousands of individuals. *Nature*, *603*(7902), 654–660. https://doi.org/10.1038/s41586-022-04492-9

Martins, B., Ponzio, A., Velasco, R., Kaplan, J., & Mather, M. (2014). Dedifferentiation of emotion regulation strategies in the aging brain. *Social Cognitive and Affective Neuroscience*, *10*(6), 840–847. https://doi.org/10.1093/scan/nsu129

McRae, K., Hughes, B., Chopra, S., Gabrieli, J. D. E., Gross, J. J., & Ochsner, K. N. (2010). The neural bases of distraction and reappraisal. *Journal of Cognitive Neuroscience*, *22*(2), 248–262. https://doi.org/10.1162/jocn.2009.21243

Misaki, M., Kim, Y., Bandettini, P. A., & Kriegeskorte, N. (2010). Comparison of multivariate classifiers and response normalizations for pattern-information fMRI. *NeuroImage*, *53*(1), 103–118. https://doi.org/10.1016/j.neuroimage.2010.05.051

Mitchell, D. G. V. (2011). The nexus between decision making and emotion regulation: A review of convergent neurocognitive substrates. *Behavioural Brain Research*, *217*(1), 215–231. https://doi.org/10.1016/j.bbr.2010.10.030

Miyake, A., Friedman, N. P., Emerson, M. J., Witzki, A. H., Howerter, A., & Wager, T. D. (2000). The unity and diversity of executive functions and their contributions to complex "frontal lobe" tasks: A latent variable analysis. *Cognitive Psychology*, *41*(1), 49–100. https://doi.org/10.1006/cogp.1999.0734

Morawetz, C., Bode, S., Baudewig, J., Jacobs, A. M., & Heekeren, H. R. (2016). Neural representation of emotion regulation goals. *Human Brain Mapping*, *37*(2), 600–620. https://doi.org/10.1002/hbm.23053

Morey, R. A., Dolcos, F., Petty, C. M., Cooper, D. A., Hayes, J. P., LaBar, K. S., & McCarthy, G. (2009). The role of trauma-related distractors on neural systems for working memory and

emotion processing in posttraumatic stress disorder. *Journal of Psyciatric Resilience*, *43*(8), 809–817. https://doi.org/10.1016/j.jpsychires.2008.10.014.The

Ochsner, K. N., Ray, R. D., Cooper, J. C., Robertson, E. R., Chopra, S., Gabrieli, J. D. E., & Gross, J. J. (2004). For better or for worse: Neural systems supporting the cognitive down- and up-regulation of negative emotion. *NeuroImage*, *23*(2), 483–499. https://doi.org/10.1016/j.neuroimage.2004.06.030

Ochsner, K. N., Silvers, J. A., & Buhle, J. T. (2012). Functional imaging studies of emotion regulation: A synthetic review and evolving model of the cognitive control of emotion. *Annals of the New York Academy of Sciences*, *1251*, 1–24. https://doi.org/10.1111/j.1749-6632.2012.06751.x.Functional

Olson, I. R., & Berryhill, M. (2009). Some surprising findings on the involvement of the parietal lobe in human memory. *Neurobiology of Learning and Memory*, *91*(2), 155–165. https://doi.org/10.1016/j.nlm.2008.09.006

Op de Beeck, H. P. (2010). Against hyperacuity in brain reading: Spatial smoothing does not hurt multivariate fMRI analyses? *NeuroImage*, *49*(3), 1943–1948. https://doi.org/10.1016/j.neuroimage.2009.02.047

Opitz, P. C., Gross, J. J., & Urry, H. L. (2012). Selection, optimization, and compensation in the domain of emotion regulation: Applications to adolescence, older age, and major depressive disorder. *Social and Personality Psychology Compass*, *6*(2), 142–155. https://doi.org/10.1111/j.1751-9004.2011.00413.x

Opitz, P. C., Lee, I. A., Gross, J. J., & Urry, H. L. (2014). Fluid cognitive ability is a resource for successful emotion regulation in older and younger adults. *Frontiers in Psychology*, *5*(JUN), 1–13. https://doi.org/10.3389/fpsyg.2014.00609

Pessoa, L. (2009). How do emotion and motivation direct executive control? *Trends in Cognitive Sciences*, *13*(4), 160–166. https://doi.org/10.1016/j.tics.2009.01.006

Poldrack, R. A. (2008). The role of fMRI in Cognitive Neuroscience: where do we stand? In *Current Opinion in Neurobiology* (Vol. 18, Issue 2, pp. 223–227). https://doi.org/10.1016/j.conb.2008.07.006

Power, J. D., Mitra, A., Laumann, T. O., Snyder, A. Z., Schlaggar, B. L., & Petersen, S. E. (2014). Methods to detect, characterize, and remove motion artifact in resting state fMRI. *NeuroImage*, *84*, 320–341. https://doi.org/10.1016/j.neuroimage.2013.08.048

Pruessner, L., Barnow, S., & Holt, D. V. (2020). A cognitive control framework for understanding emotion regulation flexibility. *Emotion*, *20*(1), 21–29. https://doi.org/10.1037/emo0000658.supp

Pruim, R. H. R., Mennes, M., Buitelaar, J. K., & Beckmann, C. F. (2015). Evaluation of ICA-AROMA and alternative strategies for motion artifact removal in resting state fMRI. *NeuroImage*, *112*, 278–287. https://doi.org/10.1016/j.neuroimage.2015.02.063

Satterthwaite, T. D., Elliott, M. A., Gerraty, R. T., Ruparel, K., Loughead, J., Calkins, M. E., Eickhoff, S. B., Hakonarson, H., Gur, R. C., Gur, R. E., & Wolf, D. H. (2013). An improved framework for confound regression and filtering for control of motion artifact in the preprocessing of resting-state functional connectivity data. *NeuroImage*, *64*, 240–256. https://doi.org/10.1016/j.neuroimage.2012.08.052

Schmeichel, B. J., & Tang, D. (2015). Individual differences in executive functioning and their relationship to emotional processes and responses. *Current Directions in Psychological Science*, *24*(2), 93–98. https://doi.org/10.1177/0963721414555178

Schweizer, S., Grahn, J., Hampshire, A., Mobbs, D., & Dalgleish, T. (2013). Training the emotional brain: Improving affective control through emotional working memory training. *Journal of Neuroscience*, *33*(12), 5301–5311. https://doi.org/10.1523/JNEUROSCI.2593-12.2013

Scult, M. A., Knodt, A. R., Swartz, J. R., Brigidi, B. D., & Hariri, A. R. (2017). Thinking and Feeling: Individual Differences in Habitual Emotion Regulation and Stress-Related Mood Are Associated With Prefrontal Executive Control. *Clinical Psychological Science*, *5*(1), 150–157. https://doi.org/10.1177/2167702616654688

Silvers, J. A., Weber, J., Wager, T. D., & Ochsner, K. N. (2015). Bad and worse: Neural systems underlying reappraisal of high-and low-intensity negative emotions. *Social Cognitive and Affective Neuroscience*, *10*(2), 172–179. https://doi.org/10.1093/scan/nsu043

Smith, R., Lane, R. D., Alkozei, A., Bao, J., Smith, C., Sanova, A., Nettles, M., & Killgore, W. D. S. (2018). The role of medial prefrontal cortex in the working memory maintenance of one's own emotional responses. *Scientific Reports*, *8*(1). https://doi.org/10.1038/s41598-018-21896-8

Snyder, H. R., Miyake, A., & Hankin, B. L. (2015). Advancing understanding of executive function impairments and psychopathology: Bridging the gap between clinical and cognitive approaches. *Frontiers in Psychology*, *6*(MAR). https://doi.org/10.3389/fpsyg.2015.00328

Tavares, T. P., Logie, K., & Mitchell, D. G. V. (2016). Opposing effects of perceptual versus working memory load on emotional distraction. *Experimental Brain Research*, *234*(10), 2945–2956. https://doi.org/10.1007/s00221-016-4697-2

Ullman, H., Almeida, R., & Klingberg, T. (2014). Structural maturation and brain activity predict future working memory capacity during childhood development. *Journal of Neuroscience*, *34*(5), 1592–1598. https://doi.org/10.1523/JNEUROSCI.0842-13.2014

Urry, H. L., & Gross, J. J. (2010). Emotion regulation in older age. *Current Directions in Psychological Science*, *19*(6), 352–357. https://doi.org/10.1177/0963721410388395

Wager, T. D., Atlas, L. Y., Leotti, L. A., & Rilling, J. K. (2011). Predicting individual differences in placebo analgesia: Contributions of brain activity during anticipation and pain

experience. *Journal of Neuroscience*, *31*(2), 439–452. https://doi.org/10.1523/JNEUROSCI.3420-10.2011

Wechsler, D. (2008). *Wechsler Adult Intelligence Scale--Fourth Edition (WAIS-IV) [Database record]*.

Woo, C.-W., Koban, L., Kross, E., Lindquist, M. A., Banich, M. T., Ruzic, L., Andrews-Hanna, J. R., & Wager, T. D. (2014). Separate neural representations for physical pain and social rejection. *Nature Communications*, *5*(1), 5380. https://doi.org/10.1038/ncomms6380

Woolrich, M. (2008). Robust group analysis using outlier inference. *NeuroImage*, *41*(2), 286–301. https://doi.org/10.1016/j.neuroimage.2008.02.042

Woolrich, M., Behrens, T. E. J., Beckmann, C. F., Jenkinson, M., & Smith, S. M. (2004). Multilevel linear modelling for FMRI group analysis using Bayesian inference. *NeuroImage*, *21*(4), 1732–1747. https://doi.org/10.1016/j.neuroimage.2003.12.023

Woolrich, M., Ripley, B. D., Brady, M., & Smith, S. M. (2001). Temporal Autocorrelation in Univariate Linear Modeling of FMRI Data. *NeuroImage*, *14*(6), 1370–1386. https://doi.org/10.1006/nimg.2001.0931

Worsley, K. J. (2001). Statistical analysis of activation images. *Functional MRI: An Introduction to Methods* , *14*(1), 251–270.

Yarkoni, T., Poldrack, R. A., Nichols, T. E., Van Essen, D. C., & Wager, T. D. (2011). Large-scale automated synthesis of human functional neuroimaging data. *Nature Methods*, *8*(8), 665–670. https://doi.org/10.1038/nmeth.1635

Zhou, F., Zhao, W., Qi, Z., Geng, Y., Yao, S., Kendrick, K. M., Wager, T. D., & Becker, B. (2021). A distributed fMRI-based signature for the subjective experience of fear. *Nature Communications*, *12*(1). https://doi.org/10.1038/s41467-021-26977-3

Figure 1: Typical experimental trial for the emotion regulation task.

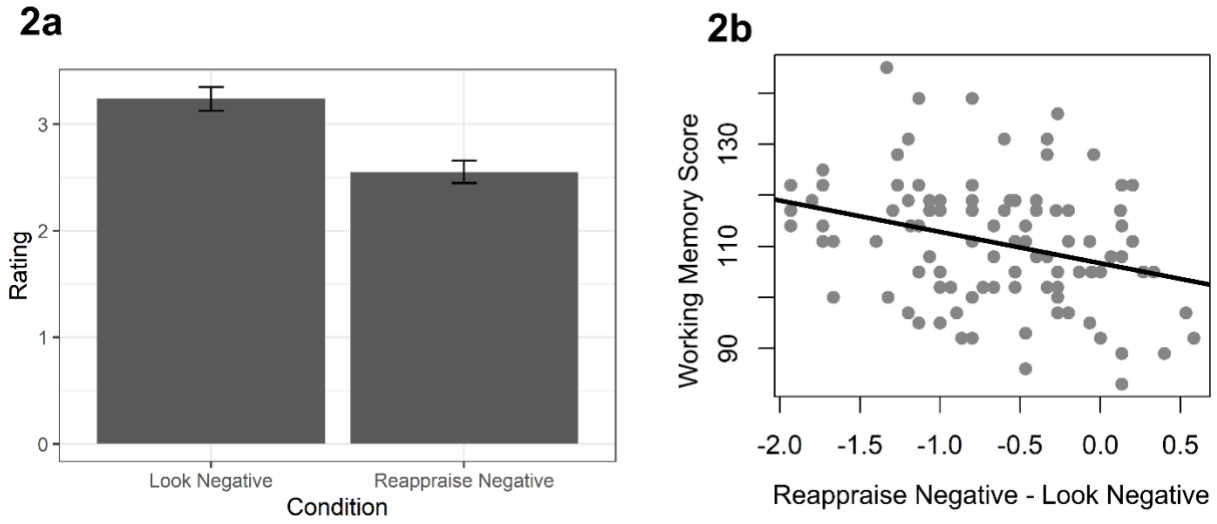

Figure 2: Behavioral results showing the difference in ratings of negativity between Look negative and Reappraise Negative conditions (Fig 2a) and correlation between Reappraise Negative – Look Negative Ratings and Working Memory score (Fig 2b)

Table 1: Significantly active clusters in differential BOLD contrast between Reappraise Negative and View Negative conditions. Clusters organized by size. Voxels represents the number of contiguous voxels in a cluster. Z-MAX is the maximum Z-value of that cluster, and the coordinates are where Z-MAX is in MNI space.

Cluster Index	Voxels	Location	Z-MAX	Z-MAX X (mm)	Z-MAX Y (mm)	Z-MAX Z (mm)
Reappraise Negative – View Negative						
1	2545	L Superior Frontal Gyrus/Middle Frontal Gyrus (DLPFC)	5.63	-4	12	64
2	2148	L Inferior Frontal Gyrus/Frontal Orbital Cortex (VLPFC)	6.39	-48	22	-22
3	1581	L Lateral Occipital Cortex	5.52	-58	-62	30
4	986	R Orbital Frontal Cortex (VLPFC)	5.98	54	36	-12
5	222	R Middle Temporal Gyrus	5.11	56	-36	0
6	205	R Frontal Pole	4.38	14	58	28
7	111	L Frontal Pole	3.96	-20	52	20
View Negative – Reappraise Negative						
1	973	L Postcentral Gyrus (Primary Somatosensory Cortex)	5.23	-50	-30	50
2	193	R Planum Temporale	4.64	54	-28	12
3	100	R Precentral Gyrus (Premotor Cortex)	4.36	40	-10	68
4	77	R Middle Temporal Gyrus/Inferior Temporal Gyrus	4.11	56	-44	-12

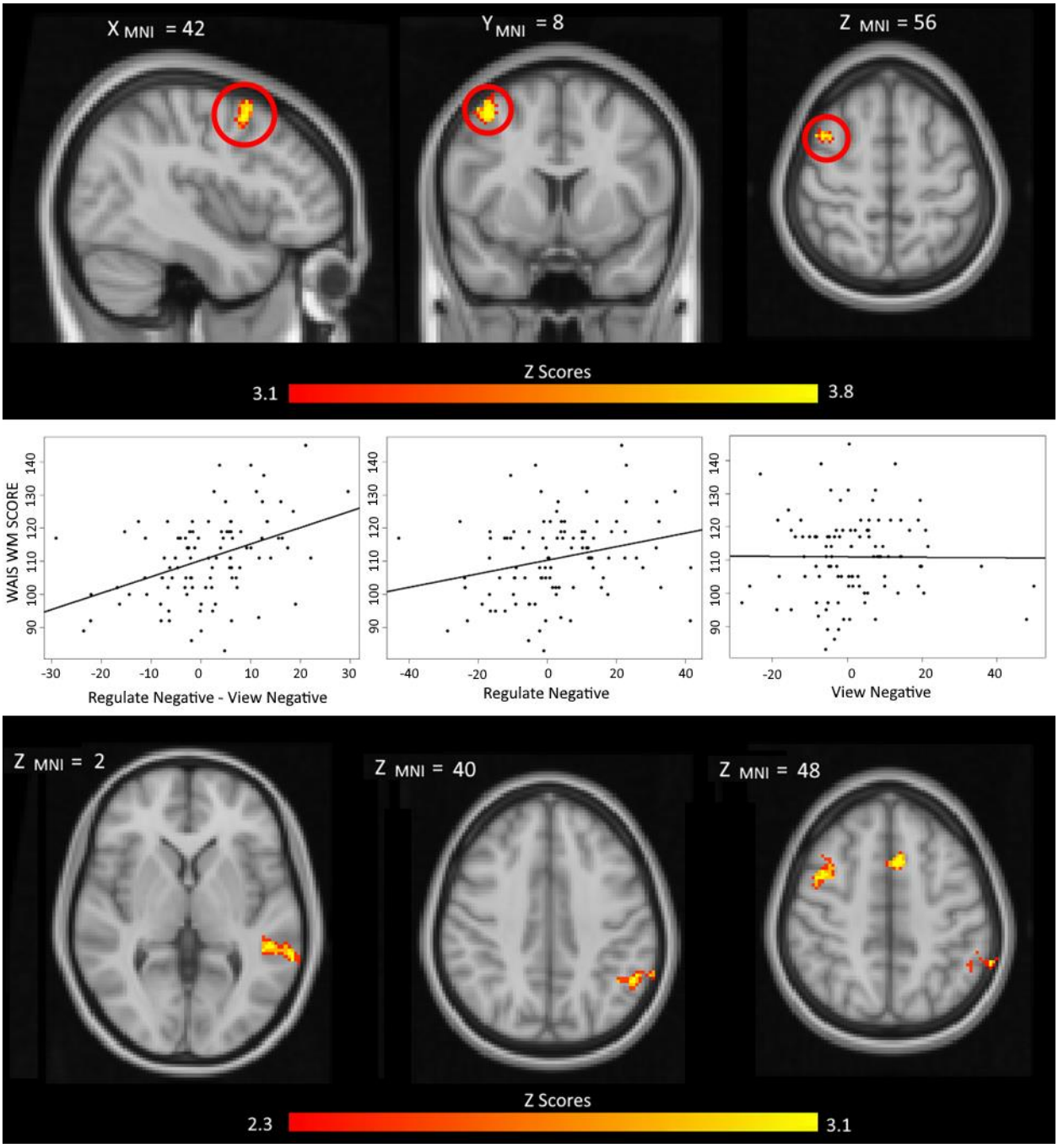

Figure 3: BOLD response of prefrontal activation predicted by working memory at a z-threshold of 3.1 (TOP), scatter plots displaying the relationship between working memory score and BOLD signal extracted from the dlPFC cluster circled in red (MIDDLE), and activation predicted by working memory at a z-threshold of 2.3 (BOTTOM). Active brain clusters are displayed on MNI 2mm brain images.

Table 2: Significantly active clusters in differential BOLD contrast between Reappraise Negative and View Negative conditions and in the Reappraise Negative condition using working memory as a predictor. Clusters noted here were based on an initial cluster threshold of 3.1 and organized by size. Voxels represents the number of contiguous voxels in a cluster. Z-MAX is the maximum Z-value of that cluster, and the coordinates are where Z-MAX is in MNI space.

Cluster Index	Voxels	Location	Z-MAX	Z-MAX X (mm)	Z-MAX Y (mm)	Z-MAX Z (mm)
Reappraise Negative – View Negative						
1	109	R Middle Frontal Gyrus (DLPFC)	4.22	42	8	56
Reappraise Negative						
1	341	L Posterior Supramarginal Gyrus	4.28	-42	-52	36
2	191	R Posterior Supramarginal Gyrus	4.67	58	-36	42
3	141	L Inferior Frontal Gyrus (DLPFC)	4.23	50	8	12

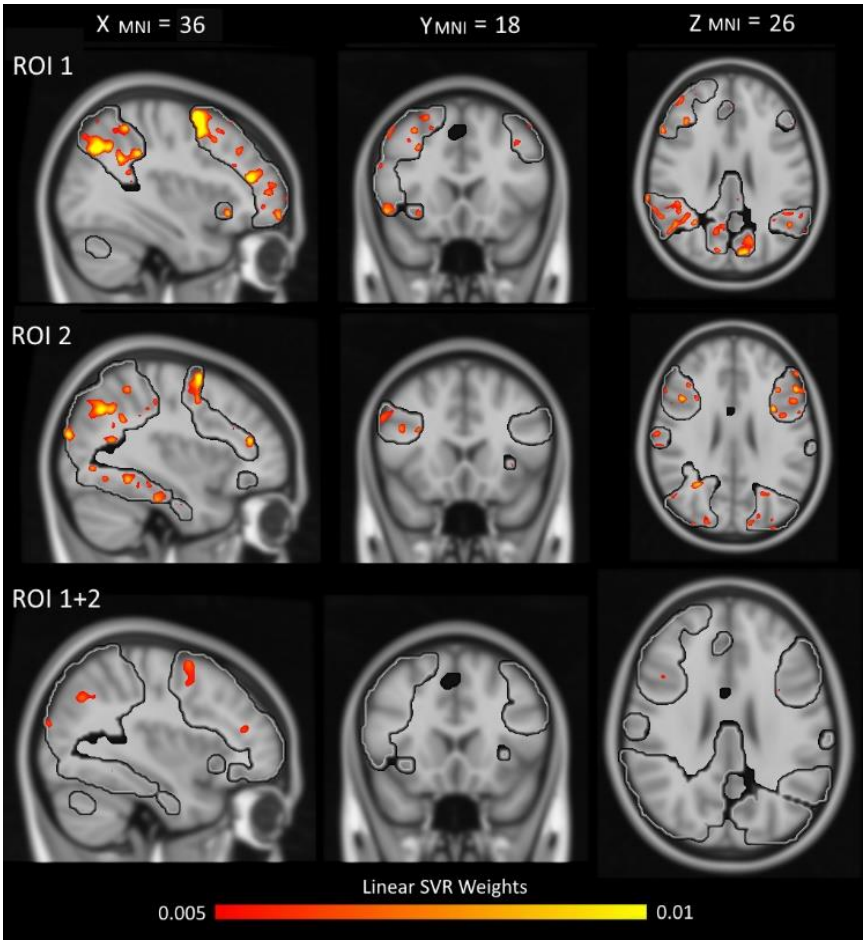

Figure 4: Weighted MVPA maps for ROI 1, ROI 2, and combined ROI maps used in multivariate analyses. The black outline denotes the area of each ROI map. Red and yellow clusters are the areas with the greatest linear weights when predicting working memory scores. Active brain clusters are displayed on MNI 2mm brain images.

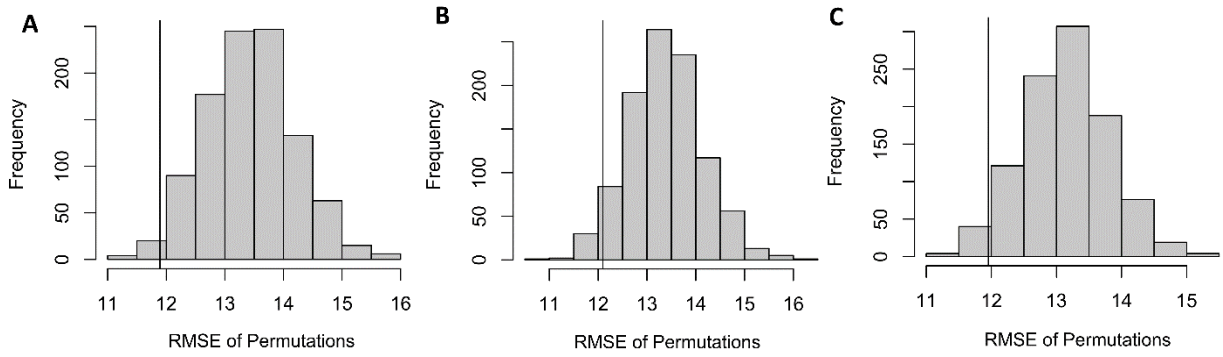

Figure 5: Histograms showing the range of permutation RMSEs for ROI 1 (A), ROI 2 (B), and the combined ROI 1 and 2 mask (C). The solid line on each histogram represents the actual RMSE of the original analysis.